F. Antón Castro, et al., Int. J. of Design & Nature and Ecodynamics. Vol. 11, No. 3 (2016) 208–219

MULTIDIMENSIONAL BIG SPATIAL DATA MODELING THROUGH A CASE STUDY: LTE RF SUBSYSTEM POWER CONSUMPTION MODELING

F. ANTÓN CASTRO[1], D. MUSIIGE[1], D. MIOC[1] & V. LAULAGNET[2]
[1]National Space Institute, Technical University of Denmark, Elektrovej 328, 2800 Kgs. Lyngby, Denmark.
[2]Micromove.com, Frederikskaj 10, 2450 Copenhagen SV, Denmark.

ABSTRACT
This paper presents a case study for comparing different multidimensional mathematical modeling methodologies used in multidimensional spatial big data modeling and proposing a new technique. An analysis of multidimensional modeling approaches (neural networks, polynomial interpolation and homotopy continuation) was conducted for finding an approach with the highest accuracy for obtaining reliable information about a cell phone consumed power and emitted radiation from streams of measurements of different physical quantities and the uncertainty ranges of these measure ments. The homotopy continuation numerical approach proved to have the highest accuracy (97%). This approach was validated against another device with a different RF subsystem design. The approach modelled the power consumption of the validation device with an accuracy of 98%.
Keywords: big spatial data, haskell, homotopy continuation, interval analysis, mathematical modeling.

1 INTRODUCTION

Comparing different multidimensional modeling methodologies is not a new research topic. It has been the main aim of the foundational work in [1]. However, in their paper, Juditsky and *et al*. [1] compared mainly neural networks and wavelets and observed that machine learning techniques exhibit the curse of dimensionality. They also observed that 'Thus wavelet based estimation algorithms are the only class of algorithms for which complete analysis is available today both for approximation and estimation'.

While homotopy continuation techniques have been used in many different fields including geodesy [2], none of these works have treated the control of the uncertainty of the homotopy continuation technique. For handling the uncertainty within the homotopy continuation, we introduce interval valued homotopies of interval vectors. In this paper, we will compare neural networks, polynomial interpolation and interval valued homotopy continuation techniques, and we will show that as we are going from neural networks to polynomial interpolation and finally homotopy continuation, these techniques are less and less subjected to an exponential growth of the number of samplings and the uncertainty of the modeling explodes less and less from one dimension to the next one. From a theoretical point of view, we know from Stone-Weierstrass approx imation theorem that any continuous function over an interval vector (i.e. over several interval variables, or more generally over a compact Hausdorff space) can be approximated uniformly to any degree of accuracy using poly nomial functions. Thus, this constitutes the theoretical justification for the polynomial interpolation as well as more specific Bernstein polynomials or splines or polynomial kernel functions. We know from Kolmogorov [3] that every continuous function on [0, 1]d can be represented as the additive

WIT CONFERENCES
This paper is part of the Proceedings of the International Conference on Big Data (Big Data 2016)
www.witconferences.com

ISSN: 1755-7437 (paper format), ISSN: 1755-7445 (online), http://www.witpress.com/journals
DOI: 10.2495/DNE-V11-N3-208-219

superposition of continuous one-dimensional functions. Therefore, this is a theoretical justification for the use of homotopies in approximation and estimation. Finally, we know that parametric statistics are based on an assumption that data satisfy some probability distribution function, while nonparametric statistics are based on the local smoothness assumption. However, in most practical cases, the data do not obey any probability distribution function and the functions we encounter are not necessarily smooth, and they present spikes, which are well represented using wavelets [4]. This is a justification for the very poor behavior of parametric statistics techniques and the poor behavior of nonparametric statistics techniques.

In this work, a new RF subsystem mathematical model that models the power consumption for all possible scenarios at any ambient temperature between −10°C and 55°C is presented. The possible scenarios are combinations of the logical interface parameter values. The main originality of this paper is the extension of the previous power emulation methodology from two-dimensional space (one variable: Tx power) to fifth-dimensional space (all logical interface parameters) keeping the uncertainty of the power emulation within the uncertainty of the validation measurements.

2 FLPA ANALYSIS OF THE RF SUBSYSTEM

The FLPA (Functional Level Power Analysis) methodology was presented in [5] for modeling the power consumption of the Systems-On-Chip (SoC). The FLPA approach is adopted in this work for finding the power consumption model of the RF subsystem. In this work, we are not only considering the high-level parameters, but also a physical environmental variable (temperature). In this section, we are applying a modified version of the FLPA analysis for finding the most optimal approach for modeling the power consumption of the RF subsystem while transmitting a LTE signal.

2.1 Primary functional analysis

The primary functional analysis of the RF subsystem, as a grey box with high-level parameters having an effective impact on power consumption, was conducted in our previous work [5]. The major power consumptions of wireless devices are largely functions of sequences of protocol/logical activities [5]. Hence, the power consumption of the RF subsystem is a function of the logical interface parameters between the RF subsystem and the DBB.

The defined extreme temperature conditions, −10°C and +55°C for the LTE technology [6], are considered in this work. The logical interface [7] parameters from the LTE technological point of view are:

- signal bandwidth ∈ {1.4, 3, 5, 10, 15, 20}MHz;
- modulation schemes *QPSK (Quadrature Phase Shift Keying)*, 16 and 64 QAM *(Quadrature amplitude modulation)*;
- Tx power ∈ [−40, 23] dBm;
- carrier frequency (depends on the supported LTE bands).

The RF subsystem power consumption is also dependent on the circumstances surrounding the near-field of the DUT (Device Under Test). Any near-field setup would have a different impedance between the antenna and PA (Power Amplifier). Each impedance is associated with a different reflection coefficient and thus, also a corresponding power consumption. In this work, the transmitter is terminated in a 50 Ω load. The effect of the near field on the power consumption of the RF subsystem is to be investigated in our proceeding work.

2.2 Device power profiling

In our previous work [5], it was proven that the power consumption of an LTE RF subsystem is technologically dependent on the carrier frequency, signal bandwidth and transmission power (Tx power). For a comprehensive study, we are also evaluating the influence of the ambient temperature. Thus, for the power profiling of the RF subsystem, the individual influence for each of the technological high level and environmental parameters on the power consumption of the RF subsystem is examined in this section.

For carrier frequency, a single band (LTE band 7) covering 2,500–2,570 MHz was considered. We are not evaluating the power consumption for the full ranges of the defined power affecting parameters as indicated in the FLPA approach. It is more efficient to define the values of the parameters at which the extrema of the power are attained and analyze the influence of the parameters in terms of the relative difference taken between the power at the lower and higher bounds as shown in Table 1.

2.2.1 Training and validation sets:

Table 1 shows that the Tx power has the biggest impact on the RF subsystem power consumption. Thus, the training and validation sets were conducted as a function of Tx power. The training sets consists of the power consumption for each combination of the lower and higher bounds of the ambient temperature, carrier frequency and signal bandwidth as a function of Tx power taken at 1 dBm resolution. The streams of measurements are conducted by an automated setup and the procedure is described as follows:

1. Three training and validation streams in room temperature ($25°C$). The DUT is cooled down for 10 min between each measurement set. It has been verified through our own experiments that the DUT takes 10 min to acclimatize to room temperature and 30 min to get to the extreme temperatures,
2. The temperature chamber is set to $-10°C$. The chamber returns the estimated time to reach the set temperature and the measurements are started after this time plus 30 min for acclimatization. Here, three training and validation streams of measurements are conducted.
3. The chamber is cooled down in 30 min and the procedure in step 2 is conducted for $55°C$.

2.3 The power consumption modeling

In this section, three multivariate modeling approaches (multivariate polynomial fitting, neural networks and homotopy continuation) are introduced and applied for modeling the power consumption of the RF subsystem.

Table 1: Parameters lower and higher bounds and significance.

Parameter	Power min	Power max	Relative diff.(%)
Carrier frequency	2,560MHz	2,510 MHz	4
Bandwidth	1.4 MHz	20 MHz	3
Tx power	−40	23	75
Temperature	−10° C	55°C	20.2

2.3.1 Multivariate polynomial fitting:

The RF subsystem power measurements, as a function of the Tx power, increases exponentially for each of the power relevant logical interface parameters, bandwidth and carrier frequency. The power consumption, as the function of the logical interface parameters, is therefore a multivariate polynomial surface known at the measured points. A function $f(w_1, ..., w_m, c_0, ..., c_{p-1}) = \sum_{k=0}^{p-1} ck\phi k\ (w_1, w_2, \ldots, w_m)$ that models the power consumption can be constructed, where p is the number of elements in the polynomial of m variables, w the function variables and c the polynomial coefficients. Without loss of generality, for a second-order bivariate polynomial model, $f(\cdot)$ becomes: $f(\mathbf{w}, \mathbf{c}) = \mathbf{c}^T \phi(\mathbf{w})$, $\mathbf{c} = [c_1, c_2, ..., c_6]^T$, $\phi(w) = [1\ w_1\ w_2\ w^2{}_1\ w^2{}_2\ w_1\ w_2]$

Given $m > K$ data points from a training data set P, where K is the number of elements in $f(\mathbf{w}, \mathbf{c})$, the coefficients $\mathbf{c}$ can be computed as $\mathrm{c} = (\Phi^{\mathrm{T}}\ \Phi)^{-1}\Phi^{\mathrm{T}}\ P$, where $\Phi \in R^{m \times K}$ is the Jacobian matrix of $\phi(x)$. However, the m variables, Tx power, signal bandwidth and carrier frequency, affecting the RF subsystem power consumption are of different lengths and the Jacobian matrix of $\Phi(x)$ cannot be used for the computation of the coefficients c. Thus, for a second-order bivariate polynomial of variables of lengths M and N, $\Phi' \in \mathrm{R}^{(\mathrm{M} \times \mathrm{N})\times K}$ for the variables bandwidth $B_{1,\ldots M}$ and Tx power $T_{1,\ldots,N}$ is constructed as:

$$\Phi' = \begin{pmatrix} B_1^d & \ldots & B_1 & B_1T_1 & T_1^d & \ldots & T_1 & 1 \\ B_2^d & \ldots & B_2 & B_2T_1 & T_1^d & \ldots & T_1 & 1 \\ \vdots & \vdots & \vdots & \vdots & \vdots & \vdots & \vdots & 1 \\ B_M^d & \ldots & B_M & B_MT_1 & T_1^d & \ldots & T_1 & 1 \\ B_1^d & \ldots & B_1 & B_1T_2 & T_2^d & \ldots & T_2 & 1 \\ \vdots & \vdots & \vdots & \vdots & \vdots & \vdots & \vdots & 1 \\ B_M^d & \ldots & B_M & B_MT_2 & T_2^d & \ldots & T_2 & 1 \\ \vdots & \vdots & \vdots & \vdots & \vdots & \vdots & \vdots & 1 \\ B_M^d & \ldots & B_M & B_MT_N & T_N^d & \ldots & T_N & 1 \end{pmatrix} \quad (1)$$

In polynomial fitting, the optimization finds the degree d for Φ' that satisfies the targeted accuracy.

2.3.2 Neural networks:

The accuracy of an approximation depends on the density of the observation points in the input space [1]. The curse of dimensionality [4] makes the accuracy of an approximation in high-dimensional spaces to require the sample size to grow exponentially with the input dimension. With the neural networks, this is solved by not having the dimension visible in the convergence rate but hidden in a functional class [1]. Given an independently measured data stream $P_t(t)$, the coefficients $W^{(1)}$ and $W^{(2)}$ can be optimized towards a minimal error between $P_t(t)$ and $P_m(t)$. The output $P_m(t)$ of the neural network is defined as:

$$P_m(t) = \sum_{j=0}^{M} W_j^{(2)} Z_j, \quad M = 1 \ldots 5,\ Z_0 \equiv 1 \quad (2)$$

$$Z_j = \sigma\left(\sum_{i=0}^{d} W_{ji}^{(1)} input_i(t)\right), \quad d = 1\ldots 4,\ input_0 \equiv 1, \tag{3}$$

where $input_i$ is the combination of the logical interface parameters at time t. The bias terms ($input_0$ for the hidden and Z_0 for output units) play an important role in ensuring that the network can represent general nonlinear mappings. The pivotal task in the neural networks is the optimization of the hidden units weights $W^{(1)}$ and the output weights $W^{(2)}$. The optimization is achieved through the minimization of the quadratic cost function (sum- of-squared errors function) between the data set Pt and the modeled power $P_m.E(W^{(1)}, W^{(2)}) = \frac{1}{2}\sum_{n=1}^{N}\left\{P_m(input_n, W^{(1)}, W^{(2)}) - Pt_n\right\}^2$

Iterative schemes taking steps in the weight space that minimize the sum-of-squared error function are utilized for finding the optimum weights. In this work, we have evaluated the following nonlinear optimization algorithms towards an algorithm with the least sum of squared errors: gradient descent; Pseudo-Gauss-Newton; conjugate gradient algorithms (Hestenes–Stiefel, Fletcher–Reeves and Polak–Ribiere).

2.4 Numerical methods using homotopy

A homotopy is a continuous deformation of geometric figures or paths or more generally functions: a function (or a path, or a geometric figure) is continuously deformed into another one [8]. Such functions or paths are then considered equivalent: i.e., homotopic. Originally, homotopy was used as a tool to decide whether two paths with same end-points would lead to the same result of integration. The use of homotopies can be tracked back to works of Poincaré (1881–1886), Klein (1882–1883) and Berstein (1910) [8].

A homotopy is defined as a continuous map between two continuous functions in a topological space. A homotopy can, therefore, be viewed as a continuous deformation. The use of deformations to solve nonlinear systems of equations may be traced back at least to Lahaye (1934) [8].

A homotopy between two continuous functions f_0 and f_1 from a topological space X to a topological space Y is defined as a continuous map $H : X \times [0, 1] \to Y$ from the Cartesian product of the topological space X with the unit interval [0, 1] to Y such that:

$$H(\mathrm{x}, 0) = f_0 \tag{4}$$

$$H(\mathrm{x}, 1) = f_1 \tag{5}$$

where $\mathrm{x} \in X$. The second parameter of H, also called the homotopy parameter, allows for a continuous deformation of f_0 to f_1 [8]. Two continuous functions f_0 and f_1 are said to be homotopic, denoted by $f_0 \cong f_1$, if, and only if, there is a homotopy H taking f_0 to f_1.

We use homotopies in order to reconstruct the unknown function of the consumed power of several power influencing variables (logical interface parameters and the physical environmental variables) from the streams of measured values obtained by fixing one variable (that will be used as homotopy parameter) and varying another variable (or possibly several other variables). In this way, we study the projections of the graph of that function of the consumed power on lower dimensional spaces (usually two dimensional spaces) corresponding to limit values of the range of the RF subsystem power influencing variable used as homotopy parameter (e.g. carrier frequency or temperature). The homotopies are specifically very strong in the modeling of continuous variables

in our case the physical environmental variable temperature. In the case of the temperature, a continuous map $H : X \times [0, 1] \rightarrow Y$ can be used to model the power consumption as a function of temperature in the defined temperature range ($-10°C$ to $+ 55°C$) [6]. The homotopy parameter λ would be set as $\lambda = 0$ and $\lambda = 1$ for the power consumptions at temperatures $-10°C$ and $+55°C$, respectively, and all the power consumptions in this range are on the homotopy curve as λ goes from 0 to 1.

The uncertainty of each measure can be represented using an interval defined either by a lower bound and a higher bound or a midpoint value and a radius. The uncertainty of the consumed power as a function of a variable (say bandwidth) can be represented by a higher bound plot and a lower bound plot. The consumed power in between the measured points can be interpolated linearly or by using cubic splines. The theoretical assumption that the consumed power is monotonically increasing with respect to the defined power influencing variables is tested by computing the intersection of the areas between the lower bound plots and the higher bound plots corresponding to the limit values of the homotopy parameter. Given that the Tx power has the most significant influence on the RF subsystem power consumption, the Tx power has to be the running variable for each of the homotopies of the other parameters. Numerically, it's always the input parameter with the widest range that is chosen as the running variable, but in our case, we also have to consider the practicality of the input parameters. Our target is the homotopy H_7 (txp, λ_{bw}, λ_{fb7} , λ_t), explained below, which computes the power consumption of the RF subsystem for any given Tx power, signal bandwidth, carrier frequency and temperature. This is achieved through a combination of homotopies for each of the power influencing parameters, as illustrated hereafter. For all these homotopies, the homotopy parameters and homotopy exponent are:

$$\lambda_{bw} = \frac{bw - 1 - 4}{20 - 1.4} \tag{6}$$

$$\lambda_{fb7} = \frac{fb7 - 2510}{2560 - 2510} \tag{7}$$

$$\lambda_t = \frac{t + 10}{55 + 10} \tag{8}$$

$$a = 1 \tag{9}$$

The homotopy continuation based computation of power consumption as a function of Tx power and signal bandwidth at the lower bound of the carrier frequency and temperature:

$$f_1 = \underset{bw,\, \underline{fb7},\underline{t}}{\underline{P_1}\left(txp\right)} \tag{10}$$

$$f_2 = \underset{\underline{bw},\underline{fb7},\underline{t}}{P_2\left(txp\right)} \tag{11}$$

$$H_2(\underset{\underline{fb7},\, \underline{t}}{\underline{txp}}, \lambda_{bw}) = (1 - \lambda bw)^a\, f_3 + \lambda_{bw}^a f_4 \tag{12}$$

The homotopy continuation based computation of power consumption as a function of Tx power and signal bandwidth at the higher bound of the carrier frequency and lower bound of temperature:

$$f_3 = \underset{bw,\, fb7,\, \underline{t}}{P_3}\left(\underline{txp}\right) \tag{13}$$

$$f_4 = \underset{\underline{bw},\, fb7,\, \underline{t}}{P_4}\left(\underline{txp}\right) \tag{14}$$

$$H_2\left(\underset{fb7,\, \underline{t}}{\underline{txp}}, \lambda_{bw}\right) = (1-\lambda bw)^{a}\, f_3 + \lambda_{bw}^{a} f_4 \tag{15}$$

The homotopy continuation based computation of power consumption as a function of Tx power and signal bandwidth at the lower bound of the carrier frequency and higher bound of temperature:

$$f_5 = \underset{\underline{bw},\, \underline{fb7},\, \bar{t}}{P_1}\left(\underline{txp}\right) \tag{16}$$

$$f_6 = \underset{\underline{bw},\, \underline{fb7},\, \bar{t}}{P_2}\left(\underline{txp}\right) \tag{17}$$

$$H_4\left(\underset{\underline{fb7},\, \bar{t}}{txp},\, \lambda_{bw}\right) = \left(1-\lambda_{bw}\right)^{a} f_5 \;+\; \lambda_{bw}^{a} f_6 \tag{18}$$

The homotopy continuation based computation of power consumption as a function of Tx power and signal bandwidth at the higher bound of the carrier frequency and temperature:

$$f_7 = \underset{\underline{bw},\, fb7,\, \bar{t}}{P_3}\left(\underline{txp}\right) \tag{19}$$

$$f_8 = \underset{\underline{bw},\, fb7,\, \bar{t}}{P_4}\left(\underline{txp}\right) \tag{20}$$

$$H_5\left(\underset{\underline{fb7},\, \bar{t}}{txp}, \lambda_{bw}\right) = \left(1-\lambda_{bw}\right)^{a} f_7 + \lambda_{bw}^{a} f_8 \tag{21}$$

The homotopy continuation based computation of power consumption as a function of Tx power, signal bandwidth, carrier frequency and temperature:

$$H_3\left(\underset{\underline{t}}{txp},\, \lambda_{bw}, \lambda_{fb7}\right) = \left(1-\lambda_{fb7}\right)^{a} H_1 \;+\; \lambda_{fb7}^{a} H_2 \tag{22}$$

$$H_6\left(\underset{\bar{t}}{txp},\, \lambda_{bw}, \lambda_{fb7}\right) = \left(1-\lambda_{fb7}\right)^{a} H_4 + \lambda_{fb7}^{a} H_5 \tag{23}$$

$$H_7\left(txp,\, \lambda_{bw}, \lambda_{fb7}, \lambda_{t}\right) = \left(1-\lambda_{t}\right)^{a} H_3 + \lambda_{t}^{a} H_6 \tag{24}$$

2.4 Evaluation of the RF subsystem power modeling approaches

This section evaluates multivariate modeling approaches towards an approach with the highest mathematical approximation accuracy. The mathematical approximation accuracy is the closeness of agreement between the modeled and measured power consumption [9]. The accuracy is computed in terms of the relative error e_r, which is between the measured power P (validation data stream) and the modelled power $\hat{P}$ i.e.,

$$e_r = \frac{\left\| P - \hat{P} \right\|_\infty}{\left\| P \right\|_\infty} \tag{25}$$

and

$$\text{accuracy} = 1 - e_r \,. \tag{26}$$

In interval analysis, each interval can be defined by a midpoint and a range. The midpoint being the most likely value of the real variable if nothing else is known or assumed about the spatial distribution of the measures. Then, the uncertainty is the range divided by 2 and the relative uncertainty is half of the range of the interval divided by the midpoint value. The absolute modeling target is to have the relative error e_r of the modeling approaches to be less than or equal to the uncertainty/precision of the measurements. The DUT was set to transmit 100 sub-frames 1,000 times at 23 dBm using 20 MHz signal bandwidth at three temperatures $-10°C$, $25°C$ and $55°C$. The precisions 5.5%, 4.5% and 5.4%, where obtained as the relative difference in each of the measurements for ambient temperatures $-10°C$, $25°C$ and $55°C$. The modeling approach(es) that will prove to have the modeling errors within the measurement uncertainties will subsequently be tried on a 'validation' prototype. This prototype is made up of the same platform as the prior but with different RF subsystem design. The major difference is that the RF subsystem of the device used in the evaluation has a different power amplifier for Lower frequency bands as band 5, high frequency bands as band 3 and 1 and band 7. Meanwhile the device to be used for validation has a single power amplifier for all bands, which means that this device should have different power consumption behaviors compared to the prior, as it has to be tuned for all the frequency bands.

2.4.1 Multivariate polynomial performance

The evaluation of the power modeling capabilities of this approach started in three dimensions for the RF subsystem power consumption as a function of signal bandwidth and Tx power. The intention was to increase the dimension if the performance proved to be within our targets. However, the evaluation of the multivariate polynomial fitting in Fig. 1 shows that this methodology can reach a minimum sum-of-squared errors of 0.19 corresponding to a relative error of 5.9% before the Φ' matrix got too close to becoming singular (hence determinant close to 0 making the Φ' matrix invertible). Thus given this performance, we can rule out the application of the multivariate polynomial fitting for the modeling of the power consumption of the RF subsystem. Finally, we have compared the relative error obtained using smoothing spline curves, thin-plate spline surfaces and piecewise linear and cubic spline surfaces with our requirement of 5%. While the relative error obtained using smoothing spline curves (3,12%) and piecewise linear and cubic spline surfaces (2,78% for both of them) are acceptable, the relative error obtained using thin plate spline surfaces is not acceptable (7,76%).

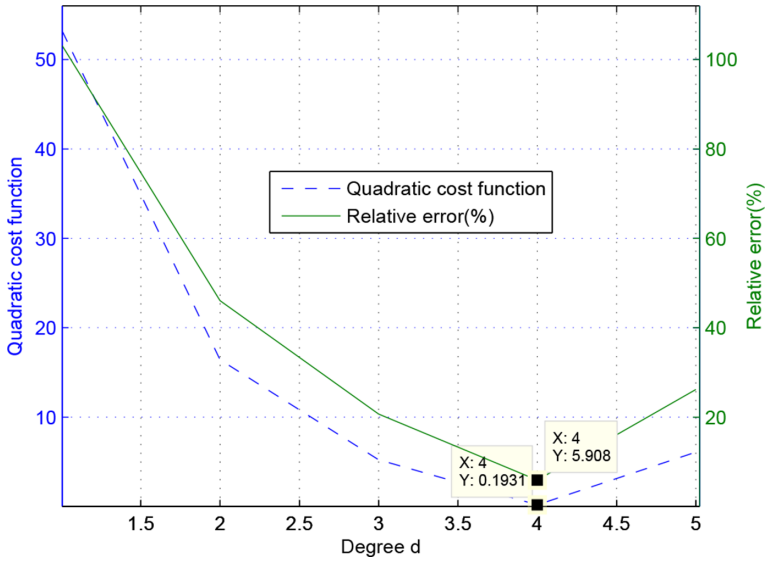

Figure 1: The performance of multivariate polynomial fitting.

2.4.2 Neural network performance

The evaluation of this approach was initiated in four dimensions for modeling the power consumption as a function of Tx power, signal bandwidth and frequency (only the lower and higher bounds of LTE band 7 were considered). The Pseudo-Gauss-Newton algorithm has the best optimization followed by Fletcher-Reeves, Polak-Ribiere with the final sum-of-squared errors 0.21, 0.30 and 0.42, respectively. This experiment was conducted for the power consumption in three-dimensional P^3. However, in the training of the neural network the weights $W^{(1)}$ and $W^{(2)}$, these weights are initialized using with pseudo-random values drawn from the standard uniform distribution. Hence, for the evaluation of the performance of this approach, the training was conducted 1,000 times yielding the following average relative errors for each of the optimization algorithms: Gradient: [51.8879, 77.5622]; Pseudo-Gauss-Newton: [6.2167, 11.8051]; Fletcher–Reeves: [6.8736, 15.5786];

Hestenes–Stiefel: [26.5198, 40.2193] and Polak–Ribiere: [8.2287, 9.8113]. These results do show that the performance of the neural networks does not fall within our target of 5%. And this is observed while considering only two carrier frequencies in band 7 and also without taking the temperature into account. Thus, to the best of our knowledge and understanding of the neural networks modeling, the approach do not meet our targeted modeling error.

2.4.3 Homotopy continuation performance

The evaluation of the performance of the homotopy continuation mapping approach initiated with four-dimensional linear homotopy (H_3 (txp, λ_{bw} , λ_{fb7}, $\underline{t}$) and H_6 (txp, λ_{bw} , λ_{fb7}, $\bar{t}$) with the intention of applying other types of homotopies accordingly in order to meet our target of the modeling error within the measurement uncertainty. The evaluation of the homotopies H3 and H6 against the validation measurement stream proved a maximum modeling error of 1.4% and 2.5% for the two homotopies, respectively. Upon the successful modeling in four dimensions (see Fig. 2), we moved to five dimensions for modeling the power consumption for any given Tx power, signal bandwidth,

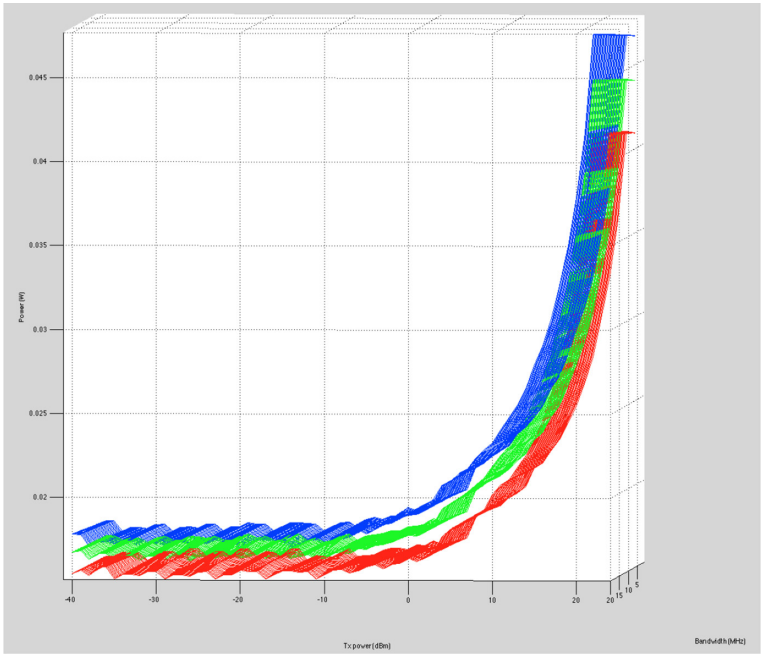

Figure 2: Plots of two bivariate homotopy functions and their intermediate trivariate homotopy.

carrier frequency (here only band 7 considered) and ambient temperature in $H_7(txp, \lambda_{bw}, \lambda_{fb7}, \lambda t)$. H_7 was evaluated against a validation stream of measurements at carrier frequencies 2,528 and 2,548 MHz, signal bandwidths 5 and 10 MHz and all Tx powers with 1 dBm resolution. The maximum relative error between the modeled power consumption and the validation set is 3%, which is within our target of 5%.

2.4.4 Modeling evaluation with a validation device

The numerical approach based on homotopy continuation has proven to have a modeling error within our measurement uncertainty. This approach was thus also put to task to model the power consumption of another design with a different RF subsystem design. For a one-to-one evaluation between the two devices, a test, where power consumption was modeled as a function Tx power operating at a signal bandwidth of 10 MHz at a carrier frequency of 2,548 MHz, was conducted. The performance of the homotopy (H_7 (txp, λ_{bw}, λ_{fb7}, λ_t)) approach on a device with a different RF subsystem design is a modeling error of 2%.

2.4.5 RF subsystem power model

The overall target in this work is to find the most accurate and efficient RF subsystem power consumption model to be applied in the power emu lator of the RF subsystem power emulation methodology introduced in [5]. In the evaluation of modeling approaches, the numerical approach homotopy continuation proved as the only one to have a modeling error within the measurement uncertainty of the five-dimensional power consumption function. Even though in our case, linear homotopy has been sufficient for both devices used in this work, there can be cases where the modeling error can appear to be out of the uncertainty bounds of the measurements. In such cases, one

would upgrade to nonlinear homotopy and subsequently linearly varying nonlinear homotopy and quadratically varying nonlinear homotopy if the prior also fails. In terms of performance, this approach has proven to have an accuracy of at least 97% evaluated over two different RF sub-system designs. For training, the approach requires eight sets of measurements $f_{1\ldots}f_8$ as a function of Tx power taken at a 1 dBm resolution (64 Tx power powers). For validation, a set of measurements for each ambient temperature,−10 °C, 25 °C and 55°C is conducted. The measurements are conducted for four carefully chosen carrier frequencies (2,510, 2,528, 2548 and 2,560 MHz in this case) for all the five operational signal bandwidths as as a function of eight carefully chosen Tx powers.

3 DISCUSSION

The implementation of the interval valued homotopy continuation has been done using the Haskell functional programming language, which is very well suited to distributed computing and concurrency. We have used lazy chunks to retrieve the streams of measurements and lazy hash-maps to store the streams of measurements. This work has focused on the modeling of the power consumption of an analog circuit, the RF subsystem, for power emulation. The power emulation methodology was introduced for digital circuits at the RTL level and was proved in a feasibility study [5] to have a precision of 10%. However, the power emulation at the RTL level cannot be conducted for realistic scenarios as for the case with the RF subsystem emulated at prototype level. Secondly, the accuracy of the emulated power at prototype level is only constrained by the accuracy of the mathematical approximation. Therefore, it is only advantageous for power analysis to also have a power emulation model of the digital circuits at prototype level. The FLPA approach would also be utilized for the computation of the emulation model of the DBB. The numerical approach based on homotopy continuation has proven to optimally conduct the functional mapping between the RF subsystem power consumption and the logical interface between the baseband and the RF subsystem for the ambient temperatures between the defined extreme cases. This modeling approach provided a mathematical function approximation accuracy of 97%. The approach was also tried on a device with a different RF subsystem design where its power consumption was modeled with an accuracy of 98%.

REFERENCES

[1] Juditsky, A., Hjalmarsson, H., Benveniste, A., Delyon, B., Ljung, L., Sjo¨berg, J. & Zhang, Q., Nonlinear black-box models in system identification: mathematical foundations. *Automatica*, **31**(12), pp. 1725–1750, 1995. http://dx.doi.org/10.1016/0005-1098(95)00119-1

[2] Palancz, B., Awange, J.L., Zaletnyik, P. & Lewis, R.H., Linear homotopy solution of nonlinear systems of equations in geodesy. *Journal of Geodesy*, **84**(1), pp. 79–95, 2010. http://dx.doi.org/10.1007/s00190-009-0346-x

[3] Kolmogorov, A.N., On the representation of continuous functions of many variables by superposition of continuous functions of one variable and addition. *American Mathematical Society Translations*, **28**(28), pp. 55–59, 1963.

[4] Bishop, C.M., *Pattern Recognition and Machine Learning*, Springer, pp. 33–38, 2006.

[5] Musiige, D., Laulagnet, V., Anton, F. & Mioc, D., LTE RF subsystem power consumption modeling. *The 1st IEEE Global Conference on Consumer Electronics 2012 (IEEE GCCE 2012)*, Tokyo, Japan, pp. 654–658, 2012. http://dx.doi.org/10.1109/gcce.2012.6379941

[6] ETSI, 3GPP Technical specification 36.101. V8.8.0 edition, (2009–12).

[7] ETSI, 3GPP Technical Specification 36.211. V8.9.0 edition, 2009.

[8] Allgower, E.L. & Georg, K., *Numerical Continuation Methods: An Introduction*. Springer-Verlag: New York, NY, USA, 1990.
http://dx.doi.org/10.1007/978-3-642-61257-2
[9] Morris, A.S. & Langari, R., Chapter 3 - measurement uncertainty. *Measurement and Instrumentation*, eds. A.S. Morris & R. Langari, Butterworth-Heinemann: Boston, pp. 39–102, 2012.